Science of the Total Environment 863 (2023) 160712

Contents lists available at ScienceDirect

Science of the Total Environment

journal homepage: www.elsevier.com/locate/scitotenv

The win-win interaction between integrated blue and green space on urban cooling

Wen Zhou [a,*], Wei Cao [a], Tao Wu [a], Ting Zhang [b,c]

[a] College of Horticulture and Landscape Architecture, Yangzhou University, 225000, China
[b] Department of architecture and design, Polytechnic University of Turin, 10125, Italy
[c] Wuxi Taihu University, 214064, China

HIGHLIGHTS

- The integration of blue and green spaces reinforces the mutual cooling potential.
- Area, shape and NDVI do not affect the cooling effect of riverside green spaces.
- More contact with the river leads to more LST drops in the riverside green space.
- Incorporating water bodies into green spaces can lead to more LST reduction.
- The cooling heterogeneity of an urban river and influencing factors were studied.

GRAPHICAL ABSTRACT

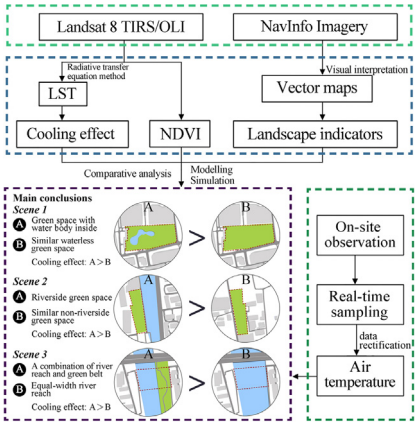

ARTICLE INFO

Editor: Paulo Pereira

Keywords:
Urban blue-green space
Combined cooling effect
Climate adaption and mitigation
Seasonal variation
Urban planning

ABSTRACT

The contributions of urban blue and green spaces on urban cooling are widely acknowledged. However, the combined cooling effect of integrated blue and green space remains uncertain. In this study, a combination of modelling and observational analyses uncovered a win–win interaction between coexisting blue and green spaces in terms of urban cooling. That is, the integration of water bodies and green spaces can reinforce the mutual cooling potential and provide greater urban cooling than stand-alone water bodies and green spaces. The results indicated that the known influencing factors such as area, shape and planting structure had no impact on the cooling effect of riverside urban green spaces. Instead, the width of the adjacent river reach and the degree of contact with the reach were significantly positively related to the cooling effect of riverside green spaces. The surface/air temperature of a riverside green space can be 4.2 °C/3.7 °C lower in the daytime in summer, and 3.1 °C/2.7 °C lower in spring than a non-riverside green space of similar size. Urban green spaces with water bodies inside could cause about 0.99 °C and 1.45 °C more deduction of land surface temperature (LST) than simple green spaces of similar size in spring and summer, respectively. There were about 1 °C-2.9 °C more deductions in the air temperature of a river reach when it is accompanied by green spaces. More specifically, complete coverage with vegetated areas within a 30 m buffer on both riverbanks can result in a 3.1 °C and 3.37 °C higher LST deduction compared to no vegetation coverage on the riverbank in the daytime in spring and summer, respectively. The results of this study extend the understanding of the cooling effect of urban blue-green spaces and provide implications for sustainable urban planning.

* Corresponding author.
E-mail address: wenzhou0305@hotmail.com (W. Zhou).

http://dx.doi.org/10.1016/j.scitotenv.2022.160712
Received 22 June 2022; Received in revised form 30 November 2022; Accepted 2 December 2022
Available online 9 December 2022

1. Introduction

The global urban share of the total population has increased dramatically from about one-third in 1950 to more than half in 2008 (Grimm et al., 2008), and is projected to reach two-thirds by 2050 (United Nations Department of Economic and Social Affairs, 2019). Rapid urbanization is accompanied by profound changes in landscape patterns and processes, such as an increase in the coverage of impervious surfaces and a decrease in blue and green spaces (Cao et al., 2016; He and Zhu, 2018; Jin et al., 2005; Rizwan et al., 2008). The increasing amount and intensity of human activities, centralization of energy consumption in urban areas, and changes in urban surface materials have led to increased anthropogenic heat production and emission (Stewart and Oke, 2003; Weng et al., 2011), causing higher temperatures in urban areas than in surrounding rural areas, which is called the Urban Heat Island (UHI) effect (Oke, 1982). The superposition of the preexisting UHI effect and climate change has led to frequent heat waves in urban areas worldwide (Corburn, 2009; Hoag, 2015; Li and Bou-Zeid, 2013), affecting the health and comfort of urban residents (Gabriel and Endlicher, 2011; Wong et al., 2016). There is growing evidence that ongoing urban warming is leading to substantial increases in human mortality from many common diseases (e.g., cardiovascular and respiratory diseases) (Anderson and Bell, 2011), morbidity (McGeehin and Mirabelli, 2001; Mora et al., 2017), energy consumption (Kusaka et al., 2012), and civil conflict (Hsiang et al., 2011), especially during heat waves (Zhao et al., 2018). As a result, mitigation and adaptation measures to the UHI effect are attracting increasing interest from both researchers and urban decision-makers.

Studies have already addressed strategies to mitigate the UHI effect from many different aspects, such as the application of cooling materials and colors (Akbari and Kolokotsa, 2016; Gilbert et al., 2016), and the development of urban blue-green infrastructure (Santamouris et al., 2018; Yu et al., 2021). Numerous studies have shown that urban blue space (i.e., lakes, reservoirs, rivers, and other bodies of water) and green space (i.e., forests, parks, green roofs, and other planted areas) can significantly reduce ambient air/surface temperatures, and provide an "urban cool island" (UCI) effect during the day (Bowler et al., 2010; Deilami et al., 2018; Koc et al., 2018; Peng et al., 2021). In particular, the UCI effect of urban water bodies is notable during the day, mainly due to their high heat capacity (i.e., they warm more slowly than the air and other materials under the same solar radiance), and evaporation and convection processes (Gunawardena et al., 2017; Manteghi et al., 2015; Zhao et al., 2017). Through evapotranspiration and shading effects, urban vegetation influences the physical environment of cities by selectively absorbing and reflecting incident radiation and regulating latent and sensible heat exchange (Rahman et al., 2017), and is defined as another effective "cold source" among the different land cover types (Bonan, 2008; Ellison et al., 2017; Lin et al., 2015; Schwaab et al., 2021). Although urban water bodies are capable of providing great cooling capacity, studies on the cooling effect of water bodies from the landscape perspective are much less than that of green space (Gunawardena et al., 2017; Koc et al., 2018; Xue et al., 2019) and mainly focused on summertime. In addition, most previous efforts focused on showing the differences between the UCI effects of different polygonal water bodies (Wang and Ouyang, 2021; Zheng et al., 2021; Zhou et al., 2021), and provided very little information on the cooling heterogeneity of an extensive river network in its different parts and the influencing factors.

The UCI effect of urban blue spaces and green spaces has been extensively documented in isolation using various cooling indicators, such as cooling intensity (Cao et al., 2010; Kong et al., 2014) and cooling distance (Bowler et al., 2010; Feng et al., 2021; Zhang et al., 2017). For example, Murakawa et al. (1991) found that the cooling distance of a 270 m wide river section of the Ota River in Hiroshima (Japan) was about 300 m, and the temperature reduction reached up to 5 °C. In Sheffield (UK), the cooling distance of a 22 m wide river did not extend farther than 30 m from the riverbank, and the daytime cooling ranged from 0.25 to 1.82 °C in the summer and spring seasons (Hathway and Sharples, 2012). Du et al. (2016) suggested that the cooling distance and intensity of water bodies are negatively correlated with their geometry, and the proportion of adjacent impervious surfaces. Cai et al. (2018) claimed that the cooling distance of water bodies in Chongqing (China) can be up to 1000 m. In Tama New Town (Japan), Ca et al. (1998) found that the cooling effect of a 60 ha park reached a distance of up to 1 km and caused a temperature reduction of 1.5 °C. Bowler et al. (2010) concluded that green spaces are able to reduce temperature by about 0.94 °C during the day and 1.15 °C at night. Yan et al. (2018) found that the cooling effect of a large park in Beijing (680 ha) was about 1.4 km from the park boundary, and was 0.6 °C to 2.8 °C cooler than the surrounding urban environment. Until now, there are still many controversies about whether urban water body or green space has a stronger cooling effect. For example, Gunawardena et al. (2017) suggested that urban green space has a greater benefit in mitigating UHI than blue space, while many other LST-based studies suggested that urban water body has a stronger cooling effect than green space (Wu et al., 2018; Yang et al., 2020; Zhou et al., 2022).

Previous studies have focused on the stand-alone cooling effect of blue space (Theeuwes et al., 2013; Zheng et al., 2021; Zhou et al., 2021) and green space (Peng et al., 2021; Yan et al., 2018; Zhou et al., 2019a) and their influencing factors, much less attention has been paid to the interactions between the co-existing water body and green space (Yu et al., 2020). Especially in southern cities of China, reservoirs are usually surrounded by forested areas, green belts are always created along watercourses, and urban parks are always a mixture of water bodies and vegetation areas (Wu et al., 2018; Yu et al., 2020). The interaction of integrated blue and green spaces on urban cooling is still uncertain, which has limited the ability to provide specific recommendations for optimizing urban land use against the UHI effect. For example, when limited land is available, the question arises whether full coverage with water, full coverage with vegetation, or a combination of blue and green spaces will have the greatest UCI effect.

To address these insufficiencies and provide implications for climate adaptation from an urban planning perspective, we take a portion of the river network of Suzhou, China—the Suzhou Moat and its riverside green spaces, as well as 134 urban green spaces (not riverside), as a case study to (1) investigate the effects of co-existing water bodies on the cooling effect of urban green spaces; (2) quantify the cooling heterogeneity of different river segments and assess the key influencing factors; and (3) determine the contribution of adjacent green spaces to the thermal environment of river reach. In addition, possible policy recommendations for urban blue-green space planning in Suzhou and other water-rich cities were proposed to better mitigate the UHI effect.

2. Materials and methods

2.1. Study area and site description

The study was conducted in Suzhou (119°55′-121°20′E, 30°47′-32°02′N), which is geographically located in east China's Jiangsu Province, bordering Shanghai to the east, Zhejiang Province to the south and the Yangtze River to the north (Fig. 1(a)). Suzhou has a typical subtropical humid monsoon climate with four distinct seasons, mild climate and abundant rainfall. The average annual temperature in 2019 was 17.6 °C and the average annual precipitation was 1120.9 mm (Suzhou Local Chronicles Compilation office, 2022). The city is located above an alluvial plain with an average elevation of about 3.5 to 5 m above sea level (Suzhou Local Chronicles Compilation office, 2022). Suzhou metropolitan area includes six urban districts and four county-level cities, with a total area of about 8657.32 km^2, and a permanent resident population of about 10.7499 million at the end of 2019 (Suzhou Municipal Bureau Statistics, 2020). It is a representative canal city of Asia, as nearly 36.6 % of the city's area is covered by water. There are >20,000 river courses and 300 lakes of different sizes (e.g., Taihu Lake, Yangcheng Lake, Yangtze River, Beijing-Hangzhou Canal), making the city one of the most water-rich destinations in China (Suzhou Municipal Bureau Statistics, 2020).

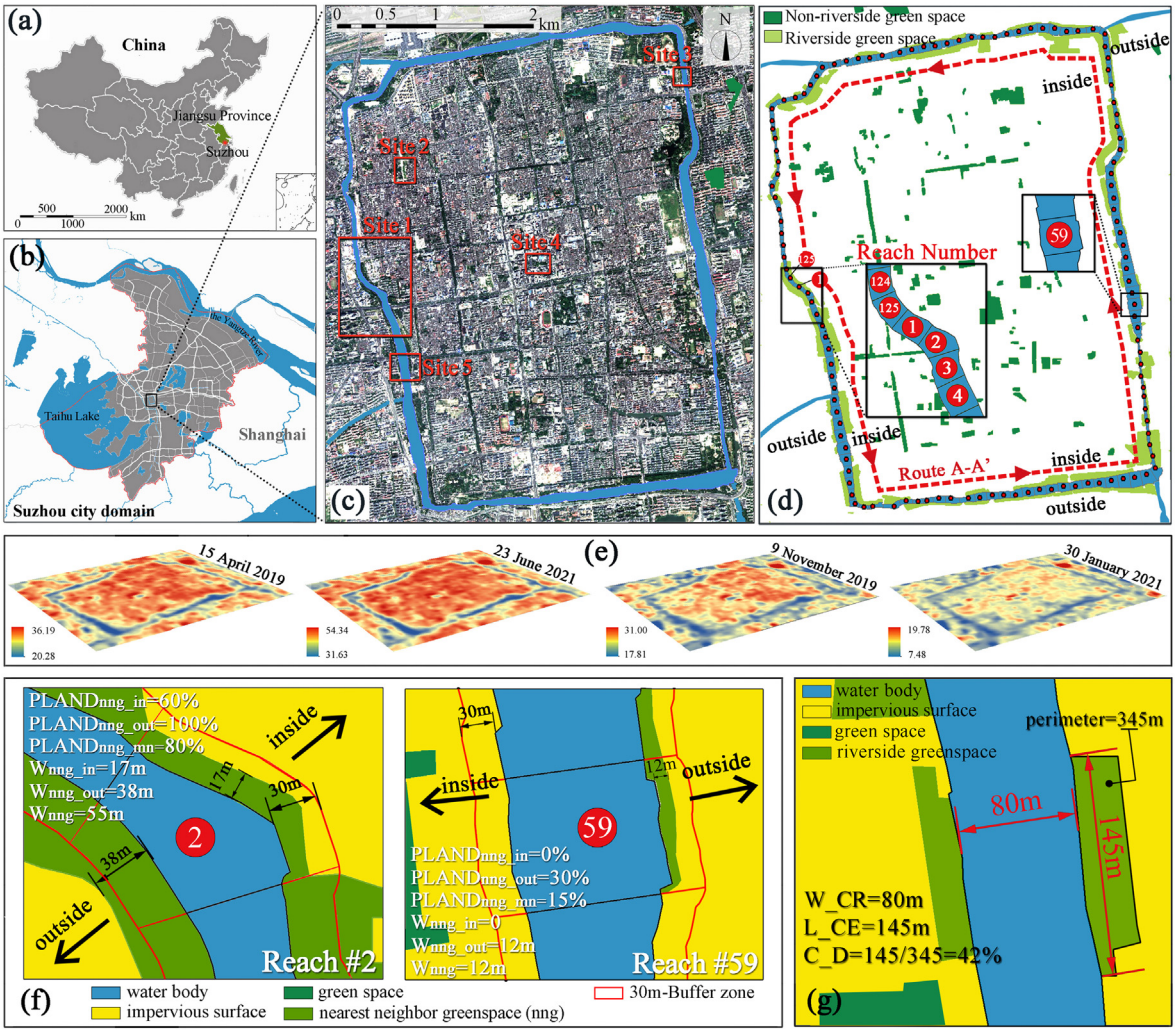

Fig. 1. Maps showing (a) the location of Suzhou city, (b) the location of the study area, (c) the satellite image of the study area and the locations of the five observation sites, (d) the river studied (reaches numbered 1–125) and the urban green spaces categorized as riverside and non-riverside, (e) distributions of land surface temperature at the four time points, (f) diagrams of $PLAND_{nng\_in}$, $PLAND_{nng\_out}$, $PLAND_{nng\_mn}$, W_{nng_in}, W_{nng_out} and W_{nng}, and (g) a diagram of W_CR (the width of the contacted reach), L_CE (the length of the edge contacted with the reach) and C_D (the degree of contact with the reach) of the riverside green space.
Note: $PLAND_{nng\_in}$ and $PLAND_{nng\_out}$ are the percentages of inside and outside nearest neighbor greenspace within the 30-m buffer zone outside the river edge, and $PLAND_{nng\_mn}$ is the average of $PLAND_{nng\_in}$ and $PLAND_{nng\_out}$. W_{nng_in} and W_{nng_out} are the transverse widths of the inside and outside nearest neighbor greenspace, and W_{nng} is the sum of W_{nng_in} and W_{nng_out}.

This study focused on the Suzhou city moat and its riverside green spaces (59 patches), which are located in the old town and city center of Suzhou and have an average altitude of about 3.5 m (120°36′-120°38′E, 31°17′-31°20′N) (Fig. 1(b)). The Suzhou city moat is a large inner-city river with an area of 1.01 km^2 and a length of about 15,400 m, with maximum and average widths of 155 m and 65 m, respectively (Fig. 1(c)). The average flow velocity is not >0.1 m/s and therefore was not considered in this study. The entire river was divided into 125 equal sections, each approximately 120 m long, and designated as Reach 1 through Reach 125 of Route A-A to quantify the heterogeneity of cooling between the different sections (Fig. 1 (d)). Because the spatial grid of the remote sensing data is 30 m, the division scale was chosen as an integer multiple of 30 m. Since the normality of two important landscape indicators (i.e., the transverse width of the reach and the percentage of the nearest neighboring greenspace of the reach) was well ensured, 120 m was selected as the division scale in this study. In addition, the cooling effects and influencing factors of 134 urban green spaces that are not located near a water body (hereafter referred to as non-riverside green spaces) were investigated to compare the difference with green spaces near water bodies (hereafter referred to as riverside green spaces) in terms of urban cooling. Thirty of 134 non-riverside green spaces were a combination of water bodies and planted area (hereafter referred to as green spaces with water body), and the rest had no water body inside (hereafter referred to as green spaces without water body). These urban green spaces mainly included urban parks, unit green spaces, private gardens, and roadside green spaces, ranging in area from 0.09 ha to 4.7 ha.

2.2. Satellite data description and processing

The data used in this study include four cloud-free Landsat-8 OLI (Operational Land Imager) images with multiple spectral bands (30 m resolution) and one panchromatic band (15 m resolution), as well as TIRS (Thermal Infrared Sensor) images (30 m resolution), and high-resolution NavInfo images. Landsat-8 OLI/TIRS images were acquired from the United States Geological Survey (https://glovis.usgs.gov/). Detailed information is provided in Table 1. Four Landsat-8 images were each acquired from one distinct season including April 15, 2019, June 23, 2021, November 9, 2019 and January 30, 2021. The OLI data were used to calculate the NDVI (Normalized Difference Vegetation Index); the TIRS imagery was used to create land surface temperature (LST) maps, and the NavInfo

Table 1
Descriptions of the Landsat 8 OLI/TIRS images used.

Seasons	Scene ID	Acquisition date	Acquisition time (BJT)
Spring	LC81190382019105LGN00	April 15, 2019	10:30 am
Summer	LC81190382021174LGN00	June 23, 2021	10:31 am
Autumn	LC81190382019313LGN00	November 9, 2019	10:31 am
Winter	LC81190382021030LGN00	January 30, 2021	10:31 am

BJT, Beijing time.

imagery was used to create vector maps of the landscape by manual interpretation, combined with ground-truthing as necessary.

The LST was calculated using the radiative transfer equation (RTE) method (Fig. 1 (e)). The principle of the RTE method is to simulate the atmospheric effects on the surface thermal radiation and subtract this atmospheric influence from the total thermal radiation observed by the satellite sensor to obtain the intensity of surface thermal radiation and then convert it to LST (Jiménez-Muñoz et al., 2014). The LST can be retrieved using Eqs. (1), (2) and (3) as follows:

$$L_\lambda = [\varepsilon B(T_S) + (1\text{-}\varepsilon)L\downarrow]/\tau + L\uparrow \quad (1)$$

where L_λ represents the thermal radiation intensity of the thermal infrared band; $B(T_s)$ is the ground radiance; ε is the surface emissivity; $L\uparrow$ and $L\downarrow$ are upward radiance and downward radiance, respectively; τ represents the atmospheric transmissivity. According to Plank's law, $B(T_s)$ can be calculated as:

$$B(T_S) = [L_\lambda - L\uparrow - \tau(1-\varepsilon)L\downarrow]/\tau\varepsilon \quad (2)$$

$$T_S = K_2/ln(K_1/B(T_S) + 1) \quad (3)$$

where T_s is the LST; For the Landsat-8 TIRS band 10, K_1 and K_2 are 774.89 ($Wm^{-2}sr^{-1}\mu m^{-1}$) and 1321.08 K (i.e., Kelvin degree), respectively.

2.3. Indicators of cooling effect

In this study, we used the mean LST and the cooling distance (CD) as indicators to quantify the cooling effect of urban blue-green space, where a lower mean LST and a greater cooling distance mean a stronger cooling effect. Same with Previous studies (Cao et al., 2010; Li et al., 2015; Sun and Chen, 2012; Yu et al., 2017), the maximum cooling distance of a river reach was defined as the distance between the boundary of the reach and the first turning point of LST. As shown in Fig. 2, a cross-sectional profile of LST of each reach was constructed to determine the cooling distance on the inside (CD_{in}) and outside (CD_{out}) directions. In this study, the temperature difference (TD) between the entire study area (water bodies excluded) (Fig. 1(c)) and the river was calculated to quantify the cooling intensity of the river in different seasons (Kong et al., 2014; Zhou et al., 2022). Therefore, greater TD means greater cooling intensity and vice versa.

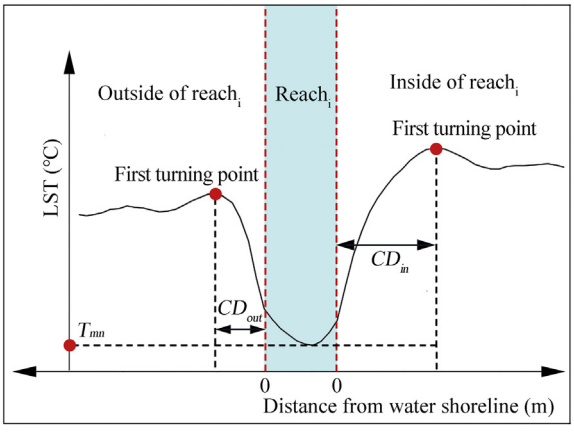

Fig. 2. The conceptual curve of CD_{in} and CD_{out}.

2.4. Selections and definitions of landscape indicators

In this study, several easy-to-use landscape indicators were used to better examine the effects of reach width and neighboring green space on the cooling effect of different river segments, including the width of reach (W_r), the percentage of inside ($PLAND_{nng\_in}$) and outside nearest neighbor greenspace ($PLAND_{nng\_out}$) within the 30-m buffer zone outside the river edge, the transverse width of the inside (W_{nng_in}) and outside nearest neighbor greenspace (W_{nng_out}) (Fig. 1(f)), and the Normalized Difference Vegetation Index of the nearest neighbor green space ($NDVI_{nng}$) which can effectively reflect the abundance of vegetation, were selected based on previous research, data availability and planning relevance. Here, the nearest neighbor greenspace (nng) refers to the green spaces that are directly contacted with the river reach. In addition, $PLAND_{nng\_mn}$ is the average of $PLAND_{nng\_in}$ and $PLAND_{nng\_out}$, and W_{nng} is the sum of W_{nng_in} and W_{nng_out}. A high NDVI value usually refers to a multi-layered planting structure and a relatively low NDVI value refers to a simpler layer. This means that the NDVI value of a tree-dominated green space is always larger than that of a grass-dominated one, so it was selected as a landscape indicator to measure the effect of planting structure on the cooling effect of urban green space.

Three common landscape indicators, including the patch area, shape index (SI = 0.25 perimeter/√Area; SI = 1 when the patch is square or nearly square and increases without limit as patch shape becomes more irregular) (Yu et al., 2017; Zhou et al., 2019b), and the mean NDVI of green space patch were calculated, and their relationships with LST of two categories of urban green spaces (riverside and non-riverside green spaces) were investigated and compared. In addition to having lower air/surface temperatures than their surroundings (Fan et al., 2019; Gomez-Martinez et al., 2021; Yan et al., 2018; Yu et al., 2018), urban water bodies and green spaces can also cool their immediate surroundings (Bowler et al., 2010; Feng et al., 2021; Zhang et al., 2017). We assumed that the cooling effect of riverside green space is influenced by the water body in contact with them. Therefore, in this study, the width of the contacted reach (W_CR), the length of the edge contacted with the reach (L_CE) and the degree of contact with the reach (C_D; corresponding to the ratio of L_CE (m) to the patch perimeter (m)) of the riverside green space (Fig. 1(g)) were introduced to quantify the impact of the adjacent water body on the patch LST of the riverside green spaces. See Supplemental Table 1 (Part II) for definitions of landscape indicators.

2.5. Statistical analysis

All statistical analyses were performed with SPSS 23.0 (SPSS Inc., Chicago, IL, USA). Pearson correlation analysis and regression analysis were performed to analyze the relationships between selected landscape indicators and cooling indicators for blue and green spaces. The stepwise multiple linear regression method (SW-MLR) was further applied to eliminate multiple collinearity and elucidate the combined effect of landscape indicators on LST variations of river segments. The SW-MLR model works under four assumptions: (1) the dependent variable is a linear function of the explanatory variables; (2) independence of the residual; (3) normality of the residual; and (4) homogeneity of the variance of the residual; and if any of the above assumptions is violated, the SW-MLR model is not fit. The relative weights (RW) analysis method was further applied based on the results of the SW-MLR analysis to determine the relative importance of the explanatory variables. An independent samples *t*-test was conducted to test whether there was a statistical difference between the cooling effects of riverside and non-riverside urban green spaces after controlling for the patch area, and of green spaces with and without water bodies after controlling for the patch area. The cooling distances of 125 river reaches of inside and outside directions in four seasons were also compared using the independent samples t-test.

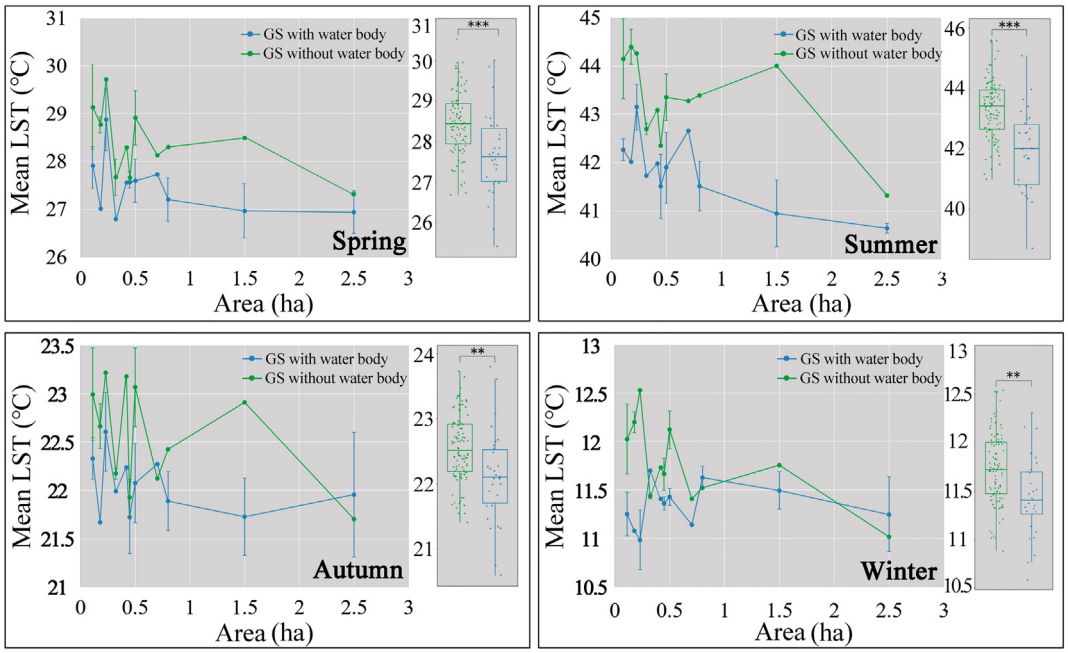

Fig. 3. Comparisons of mean LST of green spaces with and without water bodies after control for the patch area. The dots represent the mean LST (°C) values of GSs with and without water bodies. The boxes represent the 25th to the 75th percentile (IQR = interquartile range = quartile 3–quartile 1) and the upper and lower whiskers correspond to the maximum and minimum values, respectively. The line inside the box is the median value. ** and *** indicate significantly different means based on an Independent-Sample *t*-test at 0.01 and 0.001 levels, respectively.

3. Results

3.1. Impact of coexisting water bodies on LST of urban green spaces

Take all green spaces with water bodies as reference and then filter out similar-sized green spaces without water bodies for further comparison. The results showed that the mean LST of green spaces with water bodies was significantly lower than green spaces without water bodies in four seasons ($p < 0.01$) (Fig. 3). After controlling for the influence of patch area, only the means LST of green spaces with water bodies in summer and spring were consistently lower than green spaces without water bodies of similar size, indicating that the positive effect of water bodies on LST reduction of green spaces in summer and spring was more stable and significant. More specifically, the average LST difference between green spaces with and without water bodies after controlling for patch area was 1.45 °C in summer and 0.99 °C in spring.

Fig. 4 shows the mean LST of riverside green spaces and non-riverside green spaces in different areas. The results indicated that the mean LST of

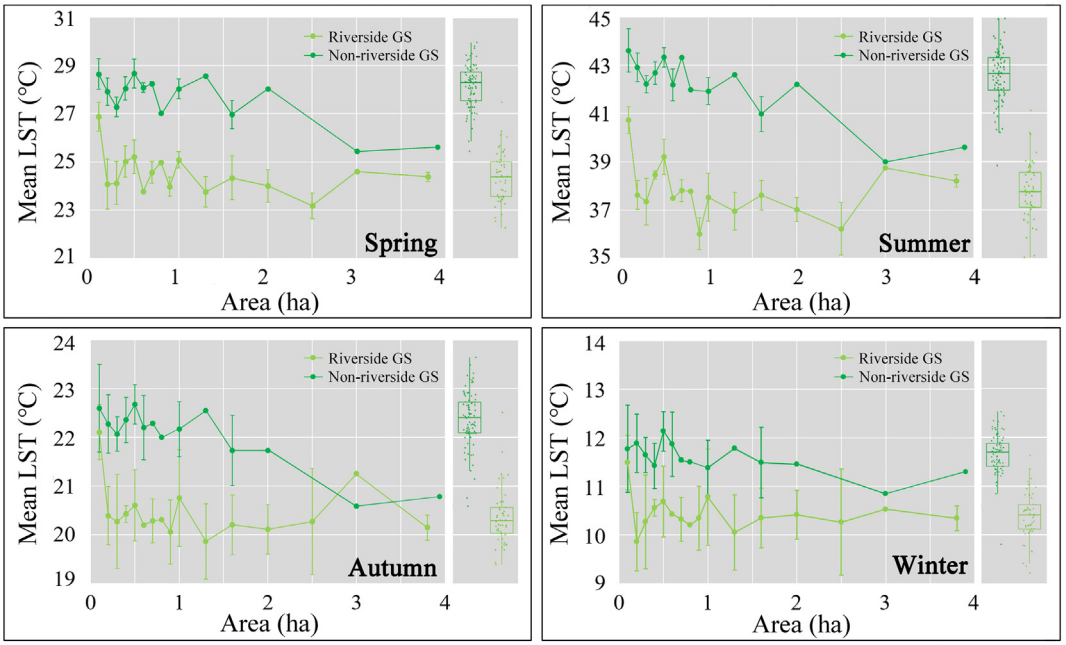

Fig. 4. Comparisons of mean LST of riverside and non-riverside urban green spaces after controlling for the patch area. The dots represent the mean LST (°C) values of riverside and non-riverside GSs. The boxes represent the 25th to the 75th percentile (IQR = interquartile range = quartile 3–quartile 1) and the upper and lower whiskers correspond to the maximum and minimum values, respectively. The line inside the box is the median value.

Table 2
The correlation coefficients between the mean LST of riverside and non-riverside green spaces and landscape descriptors in four seasons.

Seasons	Riverside green space (n = 59)						Non-riverside green space (n = 134)		
	Area	SI	NDVI	W_CR	L_CE	C_D	Area	SI	NDVI
Spring	−0.235	−0.202	−0.226	−0.618[b]	−0.377[b]	−0.320[a]	−0.460[b]	0.097	−0.479[b]
Summer	−0.247	−0. 134	−0.282	−0.608[b]	−0.439[b]	−0.438[b]	−0.525[b]	−0.013	−0.482[b]
Autumn	−0.214	−0.206	−0.232	−0.494[b]	−0.290[a]	−0.132	−0.445[b]	0.100	−0.384[b]
Winter	0.067	−0.187	−0.014	−0.483[b]	−0.025	−0.031	−0.202[a]	0.009	0.014

Note: SI and NDVI refer to shape index and Normalized Difference Vegetation Index, respectively. W_CR, L_CE and C_D are the width of the contacted reach, the length of the edge contacted with the reach and the degree of contact with the reach of the riverside green space, respectively.
[a] Correlation is significant at the 0.05 level (2-tailed).
[b] Correlation is significant at the 0.01 level (2-tailed).

riverside green spaces in spring and summer were all lower than non-riverside green spaces of similar size. Specifically, after controlling for patch area, the average difference of LST between riverside and non-riverside green spaces was largest in summer (4.2 °C), followed by spring (3.1 °C), autumn (1.6 °C) and winter (1.1 °C). In addition, the LST difference between riverside and non-riverside green spaces of similar size could be up to 5.7 °C, 4.8 °C, 2.7 °C, and 2.0 °C in summer, spring, autumn, and winter, respectively. Comparing the two categories of urban green spaces, it is found that the mean LST of non-riverside green spaces decreases as the area increases. For riverside green spaces, no clear trend was observed between the patch area and mean LST, suggesting that the thermal environment of riverside green spaces is more vulnerable to other factors rather than area.

The correlation coefficients (r) between the mean LST of urban green spaces and the associated landscape descriptors were calculated and presented in Table 2. The results indicated that the three recognized patch-level influencing factors (area, shape complexity, and NDVI) have different effects on the mean LST of riverside and non-riverside green spaces. The results confirmed that patch area was negatively correlated with the mean LST of non-riverside green space (r = −0.202 to −0.525, $p < 0.05$), but no correlations were observed between patch area and the mean LST of riverside green spaces in four seasons. Similarly, NDVI was an important factor affecting the patch LST of non-riverside green spaces in summer, spring, and autumn, but was irrelevant to the mean LST of riverside green spaces. The effect of shape complexity on the cooling effect of green spaces remained controversial, and in this case, correlations between SI and patch LST were not found for either category of urban green space. Importantly, the results confirmed the considerable impact of the adjacent water body on the thermal environment of the riverside green spaces. In particular, W_CR was able to explain more LST variation of riverside green spaces than L_CE and C_D, and its significant negative correlations with LST suggested that the cooling effect of green space adjacent to a wider river or larger water body is stronger than that of a similar green space but adjacent to a narrower river or smaller water body. Also, the negative correlations between L_CE and C_D with the mean LST of riverside green spaces indicate that the cooling effect of a riverside green space can be enhanced by increasing contact with the adjacent water body.

3.2. Quantification of cooling distances of river segments: spatial heterogeneity and influencing factors

As shown in Fig. 5, the cooling distances of 125 river reaches from the boundary to the inside and outside surroundings differed greatly in spatial perspectives. The results showed that CD_{in} of reaches was significantly greater than CD_{out} ($p < 0.001$). The ranges of CD_{in} and CD_{out} were 50 m–540 m and 30 m–450 m, respectively, with mean values of 217 m and 139 m in spring; 78 m–616 m and 37 m–299 m, respectively, with mean values of 241 m and 141 m in summer; 0 m–525 m and 0 m–420 m, respectively, with mean values of 181 m and 133 m in autumn; and 0 m–523 m and 0 m–388 m, respectively, with mean values of 140 m and 102 m in winter. Overall, the cooling distance of the river was greatest in summer, followed by spring and autumn, and shortest in winter.

The seasonal correlations of CD_{in} and CD_{out} of 125 river reaches were examined respectively (Supplementary Fig. 4). Based on the results of the correlation analysis and the scatter plot, the cooling distances of the reaches between two of four dates were all significantly correlated with each other (r = 0.607–0.928; $p < 0.001$), and their positive linear relationships indicated that the reach with a large cooling distance in one season was more likely to have a large cooling distance in the other seasons, and vice versa. In general, the correlations of CD_{in} (r = 0.703–0.928; $p < 0.001$) among the different seasons were stronger than CD_{out} (r = 0.607–0.837; $p < 0.001$), suggesting that the seasonal stability of cooling was greater in the interior of an enclosed linear water body than in the exterior direction.

Pearson correlation coefficients between the cooling distance (CD_{in} and CD_{out}) of river reaches and landscape indicators (W_r, $PLAND_{nng\_in}$/$PLAND_{nng\_out}$, W_{nng_in}/W_{nng_out}) were calculated and were shown in Table 3. Specifically, $PLAND_{nng\_in}$ and W_{nng_in} are positively correlated with CD_{in}, while $PLAND_{nng\_out}$ and W_{nng_out} are positively correlated with CD_{out}. Correlations between landscape indicators and CD_{in} of river reaches are stronger than with CD_{out} in the four seasons. Significant and negative relationships were found between cooling distance and mean LST of reaches in four seasons (r = −0.338 to −0.579; $p < 0.001$), suggesting that reach with lower LST tends to have greater cooling distance. Overall,

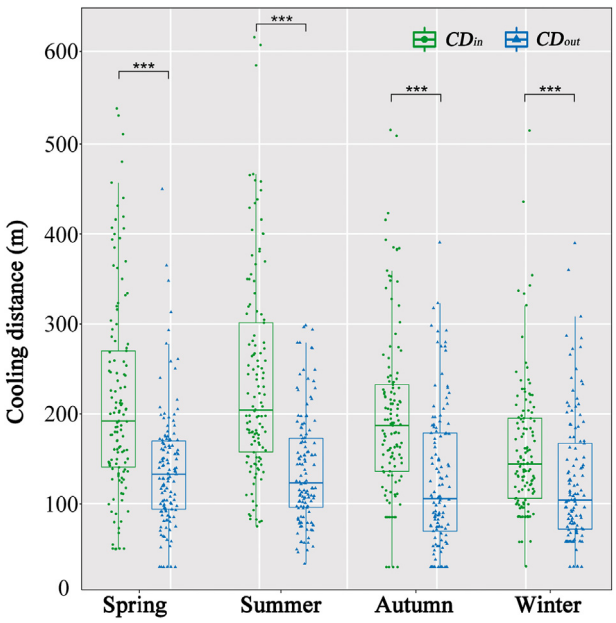

Fig. 5. The cooling distances of 125 river reaches of inside and outside directions in four seasons. The dots represent the cooling distances (m) of river reaches. The boxes represent the 25th to the 75th percentile (IQR = interquartile range = quartile 3–quartile 1) and the upper and lower whiskers correspond to the maximum and minimum values, respectively. The line inside the box is the median value. ***indicate significantly different means based on an Independent-Sample *t*-test at 0.001 level.

Table 3
Correlation coefficients between cooling distance and landscape indicators.

	W_r	$PLAND_{nng\_in}$	$PLAND_{nng\_out}$	W_{nng_in}	W_{nng_out}	LST
Spring						
CD_{in}	0.339[b]	0.725[b]	0.046	0.536[b]	0.146	−0.579[b]
CD_{out}	0.355[b]	0.095	0.473[b]	0.089	0.426[b]	−0.525[b]
Summer						
CD_{in}	0.34[b]	0.711[b]	−0.045	0.508[b]	0.13	−0.553[b]
CD_{out}	0.122	0.046	0.534[b]	0.156	0.277[a]	−0.338[b]
Autumn						
CD_{in}	0.32[b]	0.706[b]	0.035	0.546[b]	0.162	−0.525[b]
CD_{out}	0.27[a]	0.127	0.451[b]	0.085	0.439[b]	−0.571[b]
Winter						
CD_{in}	0.259[a]	0.542[b]	0.160	0.422[b]	0.094	−0.478[b]
CD_{out}	0.287[a]	0.143	0.376[b]	0.111	0.263[a]	−0.57[b]

Note:
[a] Significance at the 0.01 level.
[b] Significance at the 0.001 level.

the amount of adjacent green space can explain more CD variations of reach than its width.

3.3. Modelling the relationship between landscape descriptors and the mean LST of reach

Table 4 shows the general information of LST for 125 reach sections, including values for minimum, maximum, range, average, median, standard deviation (STDEV) and TD. The range and standard deviation values were highest in summer, followed by spring and autumn, and lowest in winter, as was TD. The results indicated that the fluctuation and variation of LST of different river reaches was highest in summer, followed by spring, autumn and winter, confirming the seasonal heterogeneity of the cooling effect of a large urban river.

As shown in Fig. 6, the heterogeneity of LST of the different river reaches was highest in summer, followed by spring and autumn, while it was lowest in winter. Using the regression analysis, it was shown that the LST of fixed river reaches in the different seasons were linearly correlated with each other (R^2 = 0.68–0.869, $p < 0.001$), with correlations varying in magnitude and being strongest between summer and spring (R^2 = 0.869, $p < 0.001$). Consistent positive linear relationships were found between the different seasons, suggesting that the thermal environment of fixed sections of the river course was relatively stable on a seasonal scale.

The results of the sampling analyses showed that spatial heterogeneity of LST of reaches was significantly associated with W_r, $PLAND_{nng\_mn}$, W_{nng} and $NDVI_{nng}$ (Fig. 7). Linear regression analysis revealed that LST of reach had the strongest negative correlation with W_r in spring, summer and winter (R^2 = 0.56–0.58, $p < 0.001$), followed by $PLAND_{nng\_mn}$, W_{nng}, and $NDVI_{nng}$. However, the relevance between LST and the indicators of neighboring green spaces ($PLAND_{nng\_mn}$, W_{nng}, and $NDVI_{nng}$) was significantly lower in winter than in other seasons, suggesting that the width of reach was far more important than the characteristics of the surrounding vegetation patches in explaining the heterogeneity of LST in winter. Unlike

Table 4
The statistics of LST of 125 river reaches in four seasons.

	Min	Max	Range	Average	Median	STDEV	TD
Spring	20.28	27.72	7.43	23.9	23.85	1.49	4.5
Summer	31.67	42.22	10.55	36.64	36.89	2.18	6.67
Autumn	18.86	22.52	3.66	20.34	20.23	0.74	2.25
Winter	8.97	11.89	2.92	10.19	10.18	0.58	1.46

Note: TD was the difference between the mean LST of the study area, i.e., the mean LST of total grids (excluding water bodies), and the mean LST of the river. Min, Max and STDEV refer to minimum value, maximum value and standard deviations, respectively.

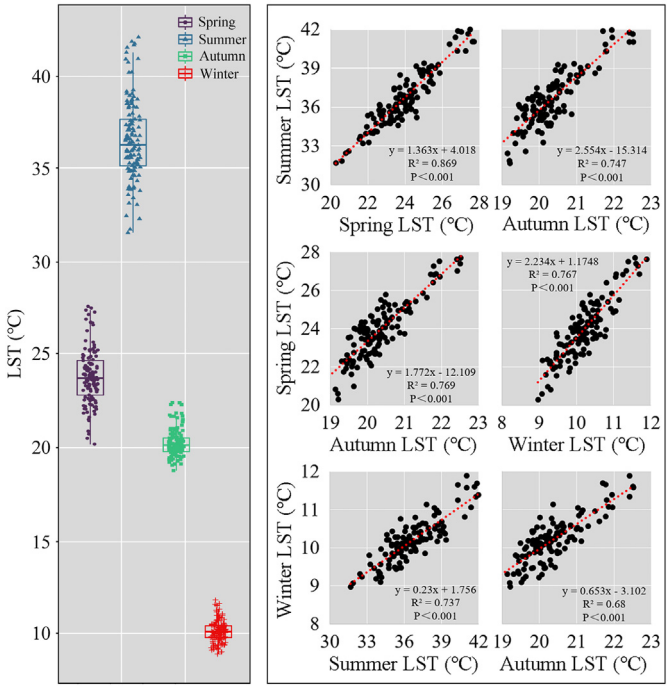

Fig. 6. (a) Distribution of mean LST of 125 river reaches in four seasons, and (b) Seasonal correlations between mean LST of fixed river reaches. The dots represent the mean LST (°C) values of 125 river reaches in four seasons. The boxes represent the 25th to the 75th percentile (IQR = interquartile range = quartile 3–quartile 1) and the upper and lower whiskers correspond to the maximum and minimum values, respectively. The line inside the box is the median value. The dotted line is the fitting curve.

other seasons, $PLAND_{nng\_mn}$ can explain much more LST variation in autumn (i.e., 50.9 %) than other landscape descriptors. According to the results of the linear regression analysis, a 10 % increase in $Pland_{nng\_mn}$ (equivalent to about 6-m-wide riverside greenspace, as the buffer size in this study was 30 m outside the reach boundary) of the water body led to a decrease in LST of about 0.32 °C, 0.49 °C and 0.19 °C in spring, summer and autumn, respectively. At the same time, increasing the W_r of the reach by 6 m resulted in a decrease of LST by about 0.22 °C, 0.32 °C and 0.08 °C in spring, summer and autumn, respectively.

Table 5 summarizes the results of the stepwise multiple linear regression (SW-MLR) analysis and the relative weights (RW) analysis. The VIF (variance inflation factor) values ranging from 0.301 to 3.638 indicated a low degree of collinearity among the variables used in this study across the four seasons. The results of Durbin-Watson test were 1.281, 1.207, 0.877 and 0.894 (between 0 and 4) for four models and normality and homoscedasticity were observed in the residuals (Supplementary Fig. 5). Overall, the results indicated that the explanatory variables included in the analysis were able to explain a significant proportion of the spatial heterogeneity of LST of different reaches in spring (R^2 = 0.804, $p < 0.001$), summer (R^2 = 0.837, $p < 0.001$), autumn (R^2 = 0.683, $p < 0.001$) and winter (R^2 = 0.648, $p < 0.001$). The results of the RW analysis provided information on the relative importance of the variables, and showed their overall contribution to the explanatory and predictive power of the regression model. Based on raw and rescaled importance, W_r had the relatively highest importance in all four seasons, followed by $PLAND_{nng\_mn}$.

4. Discussion

4.1. Enhancing effect of coexisting water bodies on the cooling effect of urban green spaces

The results of this study essentially agree that the cooling effect of larger and tree-dominated urban green spaces was stronger than that of smaller

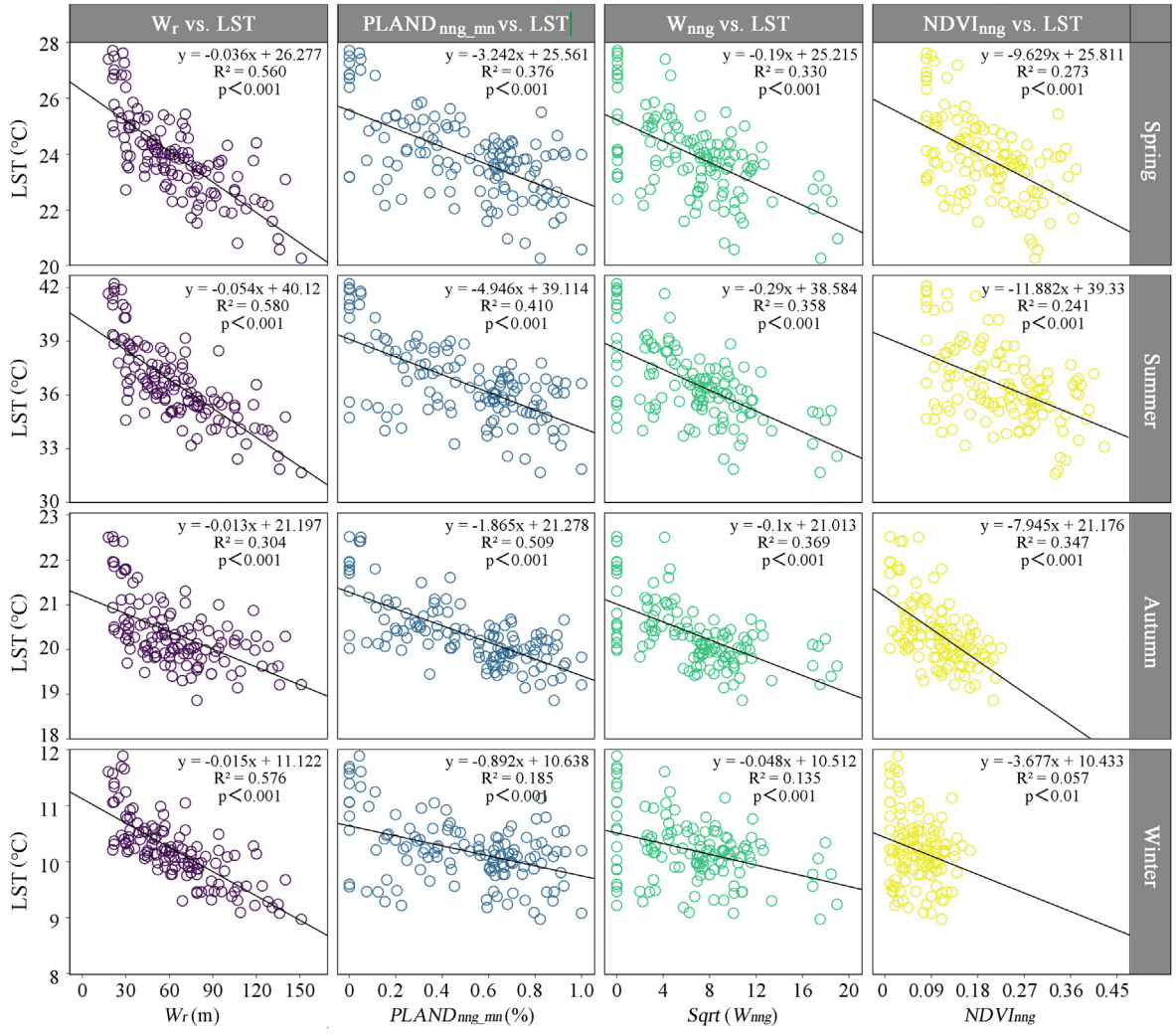

Fig. 7. Relationships between landscape variables and mean LST of reach for four seasons. The black line is the fitting curve.

and grass-dominated ones in warm and hot seasons, which is consistent with some previous studies (Myint et al., 2015; Shiflett et al., 2017; Yang et al., 2020; Zhou et al., 2022). However, the results of this study also suggest that we should be cautious about directly applying this statement to urban green spaces that directly border a water body. Based on the results of the on-site observation, the cooling intensity of a smaller grass-dominated green space on the riverbank was stronger than a larger non-riverside tree-dominated green space (Supplementary Table 1 and Supplementary Fig. 3). The results based on the data of LST also suggest that a small riverside green space could have a significant stronger cooling effect than a larger non-riverside green space (Fig. 4), indicating that patch area is not a dominant factor influencing the cooling effect of a riverside green space in this study (Table 2). Our study also confirmed that the other two well-documented patch-level influencing factors, including shape and NDVI, were no longer relevant to the cooling effect of these riverside green spaces. Instead, significant correlations were observed between the mean LST of riverside green space and the landscape descriptors associated with the adjacent reach (i.e., W_CR, L_CE and C_D in this study), suggesting that the width of the contacted reach and the degree of contact with the reach are two important aspects influencing the thermal environment of riverside green spaces.

Our study showed that riverside urban green spaces have significantly stronger cooling effect than similar-sized non-riverside urban green spaces. The temperature difference was greatest in the daytime in summer, followed by spring, and was small in autumn and winter. Specifically, the mean LST of a riverside green space can be up to 5.7 °C lower in summer and up to 4.8 °C in spring than a similar non-riverside green space, and similar but weaker patterns were observed in autumn and winter (Fig. 4). In the on-site observation, the cooling intensity of a riverside tree-dominated green space was about 2.7 °C and 3.7 °C stronger in spring and summer, respectively, than that of a similar-sized non-riverside tree-dominated green space (Supplementary Fig. 3); similar results were reported in Chongqing, China (Shi et al., 2020), where a difference of 3.3 °C was measured between littoral forest and the stand-alone forest in summer. Similarly, there were about 2.2 °C and 1.8 °C more deductions in air temperature in spring and summer, respectively, compared to a riverside grass-dominated green space and a similar-sized non-riverside grass-dominated green space (Supplementary Fig. 3). Furthermore, this study confirmed that green spaces with water bodies had significantly lower LST in spring and summer than similar-sized green spaces without water bodies. With a water body inside, the green space could generate about 0.99 °C and 1.45 °C more LST deduction in spring and summer, respectively.

4.2. Strong contribution of the neighboring green space to the cooling effect of river reach

This study confirmed the heterogeneity of cooling distances of different sections of a large river to surrounding areas from spatial, directional and seasonal perspectives. Overall, the cooling effect of the enclosed river is stronger on the inside than on the outside. Furthermore, the total cooling

Table 5
Results of the SW-MLR analyses and RW analyses (N = 125).

SW-MLR analysis							RW analysis	
Dependent variable	Variables	Unstandardized coefficients		Standardized coefficients (β)	Sig.	VIF	Raw importance	Rescaled importance (%)
		β	Std. Error					
LST_0415	(Constant)	27.454	0.204		0.000			
	W_r	−0.032	0.002	−0.652	0.000	1.089	0.560	69.65
	$PLAND_{nng\_mn}$	−1.118	0.408	−0.212	0.007	3.638	0.210	26.12
	W_{nng}	−0.003	0.001	−0.164	0.001	1.527	0.022	2.74
	$NDVI_{nng}$	−3.609	1.367	−0.196	0.009	3.357	0.012	1.49
	R^2 = 0.804; Adjusted R^2 = 0.797				***Total***		**0.804**	**100.0**
	***LST_0415* = 27.454–0.032 W_r - 1.118 $PLAND_{nng\_mn}$ - 0.003 W_{nng} - 3.609 $NDVI_{nng}$**							
LST_0623	(Constant)	41.434	0.216		0.000			
	W_r	−0.046	0.003	−0.641	0.000	1.057	0.580	69.3
	$PLAND_{nng\_mn}$	−3.008	0.350	−0.389	0.000	1.521	0.233	27.83
	W_{nng}	−0.006	0.001	−0.189	0.000	1.494	0.024	2.87
	R^2 = 0.837; Adjusted R^2 = 0.833				***Total***		**0.837**	**100.0**
	***LST_0623* = 41.434–0.046 W_r – 3.008 $PLAND_{nng\_mn}$ - 0.006 W_{nng}**							
LST_1109	(Constant)	21.829	0.102		0.000			
	W_r	−0.010	0.001	−0.435	0.000	1.090	0.509	74.52
	$PLAND_{nng\_mn}$	−1.186	0.244	−0.453	0.000	0.301	0.162	23.72
	$NDVI_{nng}$	−2.308	1.059	−0.199	0.031	0.315	0.012	1.76
	R^2 = 0.683; Adjusted R^2 = 0.675				***Total***		**0.683**	**100.0**
	***LST_1109* = 21.829–0.01 W_r - 1.186 $PLAND_{nng\_mn}$ – 2.308 $NDVI_{nng}$**							
LST_0130	(Constant)	11.332	0.084		0.000			
	W_r	−0.013	0.001	−0.698	0.000	1.052	0.576	88.89
	$PLAND_{nng\_mn}$	−0.569	0.114	−0.275	0.000	1.052	0.072	11.11
	R^2 = 0.648; Adjusted R^2 = 0.642				***Total***		**0.648**	**100.0**
	***LST_0130* = 11.332–0.013 W_r – 0.569 $PLAND_{nng\_mn}$**							

Note: Both the unstandardized coefficient estimates and the standardized coefficient estimates of the four models are reported. The standardized coefficient estimates help to determine the relative importance of the explanatory variables. The larger the absolute value of the standardized coefficient estimate, the more important the variable. *LST_0415, LST_0623, LST_1109 and LST_0130* represent the LST of 15th April 2019; 23rd June 2021; 9th November 2019 and 30th January 2021, respectively.

distance of the river sections is greatest in summer, followed by spring, autumn and winter. There were significantly positive linear relationships between cooling distances of the fixed reaches in different seasons (R^2 = 0.703–0.928, $p < 0.001$), and the most significant correlation was between summer and spring, suggesting that the results of a similar study conducted in one season may apply to others to some extent. The results of the correlation analysis showed that the width of the river reach and the riverside green space have a significant influence on the cooling distance, i.e., increasing the width of the river reach and the neighboring vegetation area can increase the cooling distance. The results suggested that the selected landscape variables could explain more spatial variation in CD_{in} than in CD_{out}, and CD_{out} may be more affected by other factors. More importantly, increasing the area of neighboring green space has a significantly stronger effect on the cooling distance than increasing the width of the reach.

Similar to the cooling distance, a seasonal correlation of mean LST of the fixed reach was observed between the different seasons (R^2 = 0.68–0.869, $p < 0.001$). Based on the means, ranges and standard deviations of LST of 125 reaches in four seasons, the spatial heterogeneity of the thermal environment of a large urban river is greatest in summer, followed by spring, and much weaker in autumn and winter. The width of reach was found to be an important factor affecting the cooling effect of water bodies, which is consistent with previous studies (Du et al., 2016; Sun et al., 2012; Wu et al., 2020; Yang et al., 2020; Zhou et al., 2022). Notably, the nearest neighbor green space-related indicators, including $PLAND_{nng\_mn}$, W_{nng}, and $NDVI_{nng}$, were all able to explain the LST variations of different river sections in four seasons, with the only exception that $NDVI_{nng}$ was not relevant to the reach LST in winter; therefore the results confirmed that the magnitude of water cooling was influenced by the surrounding landscape patterns (Hathway and Sharples, 2012; Sun and Chen, 2012; Xue et al., 2019). Results indicated that the SW-MLR model was suitable for modelling the relationship between LST of reach and selected landscape indicators in this study. The combination of these landscape indicators can explain about 79.7 %, 83.3 %, 67.5 % and 64.2 % of LST variation of reaches in spring, summer, autumn, and winter, respectively.

According to the results of linear regression analysis, the increase of $Pland_{nng\_mn}$ could lead to a greater reduction in LST of reach than the increase of W_r, indicating that the increase of the area of the nearest vegetation cover of the reach has a greater effect on urban cooling than the widening of the reach in spring, summer and autumn. Meanwhile, we also simulated two situations and compared the results based on the models from SW-MLR analyses: one is a stand-alone river section (e.g., 120 m-wide), the other is a combination of river and green belt (i.e., 60 m-wide river section with 60 m-wide riverside green spaces, 30 m-wide on each side, 120 m-wide in total). The simulation results showed that integrated blue and green space can bring about 0.1 °C and 0.61 °C more LST deduction than a stand-alone water body in spring and summer, respectively. During the on-site observation, about 1 °C–2.9 °C more deductions in the air temperature of a river section were found when it was accompanied by green space (Supplementary Fig. 2).

4.3. Limitations of the study

There are some limitations of this study that should be addressed. First, the resolution of the Landsat 8 OLI/TIRS image is limited, and therefore restricts the application of the findings based on this resolution in urban planning. In addition, the resampling of remote sensing products for data extraction could have some impact on the results, so the issue of scale should be considered. Secondly, remote sensing images are acquired instantaneously, so the conclusions depend on the time of acquisition, and should not be simply applied to other times with different climatic conditions (i.e., wind speed, wind direction and humidity). Finally, this study focused on the surface UCI effect of urban blue-green spaces, and the lack of corresponding air temperature comparisons is another limitation of this study. Meteorological data are effective predictors of thermal comfort, heat stress and heat mortality in humans, however, the relationship between the physical environment and LST is uncertain. Therefore, multi-scale studies need to be conducted covering more areas or cities with different landscape patterns and natural conditions (e.g., altitude, topography, climate, vegetation

and river system) from spatial and temporal (i.e., diurnal, seasonal and annual) perspectives.

4.4. Implications for urban blue-green space planning and design

The effect of shape of green space patches on urban cooling is still uncertain and controversial (Yu et al., 2020). Many previous studies have suggested that compact and regular green space can provide more cooling (Du et al., 2016; Feyisa et al., 2014; Masoudi and Tan, 2019), but some others hold the opposite view (Chen et al., 2014; Dugord et al., 2014; Zhou et al., 2022). However, we found that the patch shape is irrelevant to the mean LST of riverside and non-riverside urban green spaces in all seasons, so the patch shape does not need to be considered when planning urban green spaces in terms of mitigating the UHI in Suzhou. For non-riverside urban green spaces, the magnitude of cooling effect depends largely on the size and planting structure in spring, summer and autumn. Therefore, increasing the amount of vegetation and planting more trees to replace simpler-layered vegetation cover (e.g., grassland or grass-dominated areas) are effective measures to improve the cooling effect. It is noteworthy that the size, shape and planting structure do not play an important role in the planning and design of riverside or lakeshore green spaces regarding the UHI mitigation. Instead, if the area available for a green space is limited, a linear shape that has a higher degree of contact with the adjacent water body can enhance the thermal exchange between the green space and the water body, and thus achieve better cooling.

This study has shown that urban green spaces with water areas inside have a stronger cooling effect than similarly sized stand-alone green spaces in warm and hot seasons. It is therefore suggested that, where possible, water bodies should be included in the planning of urban green spaces to reduce the UHI effect. The results of this study confirmed and underlined the importance of green spaces in landscape design of the river or lake shore zone. The strongest cooling of river sections always occurs where there is high amount of vegetation cover and shading. This means that creating green spaces along a linear watercourse or river network can not only enhance the cooling effect of the green spaces, but also effectively lower the LST of the watercourse and increase its cooling distance to surroundings. In combination with the above conclusions, a green belt or linear green space is a highly recommended spatial form along an urban river to mitigate the UHI effect.

5. Conclusions

This study confirmed that the coexistence of urban green and blue spaces enhances their mutual cooling potential in mitigating the UHI effect. The study provided three main findings: 1) an urban green space with water bodies provide more LST deduction than a waterless green space of similar size; 2) the cooling effect of a riverside green space is stronger than that of a similarly sized non-riverside green space; and 3) the river-green belt combination is more effective than a single water body in urban cooling. As two important cooling sources among different land cover types, the integration of water bodies and green spaces can enhance each other's cooling potential and provide more cooling to cities than if they are distributed separately. Urban planning is a trade-off. Therefore, we suggest that more attention should be paid to the composition ratio of integrated blue and green spaces to maximize the cooling capacity of limited urban space.

CRediT authorship contribution statement

W. Z. conceived the idea and wrote the manuscript, W. Z. and W. C. conducted the analyses, T. W. and T. Z. reviewed and edited the manuscript. All authors contributed in the on-site observations and also the discussion of the results and in writing the paper.

Data availability

Data will be made available on request.

Declaration of competing interest

The authors declare that they have no known competing financial interests or personal relationships that could have appeared to influence the work reported in this paper.

Acknowledgements

This work is supported by the National Natural Science Foundation of China (Grant Number: 32101577; Representative: Wen Zhou) and Scientific Research Foundation for Advanced Talents, Yangzhou University (Grant Number: 137012167; Representative: Wen Zhou). Special thanks to three anonymous reviewers and the editor for their valuable comments to improve our manuscript.

Appendix A. Supplementary data

Supplementary data to this article can be found online at https://doi.org/10.1016/j.scitotenv.2022.160712.

References

Akbari, H., Kolokotsa, D., 2016. Three decades of urban heat islands and mitigation technologies research. Energy Build. 133, 834–842.
Anderson, G.B., Bell, Michelle L., 2011. Heat waves in the United States: mortality risk during heat waves and effect modification by heat wave characteristics in 43 US communities. Environ. Health Perspect. 119, 210–218.
Bonan, G.B., 2008. Forests and climate change: forcings, feedbacks, and the climate benefits of forests. Science (80-.) 320, 1444–1449.
Bowler, D.E., Buyung-Ali, L., Knight, T.M., Pullin, A.S., 2010. Urban greening to cool towns and cities: a systematic review of the empirical evidence. Landsc. Urban Plan. 97, 147–155. https://doi.org/10.1016/j.landurbplan.2010.05.006.
Ca, V.T., Asaeda, T., Abu, E.M., 1998. Reductions in air conditioning energy caused by a nearby park. Energy Build. 29, 83–92. https://doi.org/10.1016/S0378-7788(98)00032-2.
Cai, Z., Han, G., Chen, M., 2018. Do water bodies play an important role in the relationship between urban form and land surface temperature? Sustain. Cities Soc. 39, 487–498.
Cao, X., Onishi, A., Chen, J., Imura, H., 2010. Quantifying the cool island intensity of urban parks using ASTER and IKONOS data. Landsc. Urban Plan. 96, 224–231. https://doi.org/10.1016/j.landurbplan.2010.03.008.
Cao, C., Lee, X., Liu, S., Schultz, N., 2016. Urban heat islands in China enhanced by haze pollution. Nat. Commun. 7, 12509.
Chen, A., Yao, X.A., Sun, R., Chen, L., 2014. Effect of urban green patterns on surface urban cool islands and its seasonal variations. Urban For. Urban Green. 13, 646–654. https://doi.org/10.1016/j.ufug.2014.07.006.
Corburn, J., 2009. Cities, climate change and urban heat island mitigation: localising global environmental science. Urban Stud. 46, 413–427.
Deilami, K., Kamruzzaman, M., Liu, Y., 2018. Urban heat island effect: a systematic review of spatio-temporal factors, data, methods, and mitigation measures. Int. J. Appl. Earth Obs. Geoinf. 67.
Du, H., Song, X., Jiang, H., Kan, Z., Wang, Z., Cai, Y., 2016. Research on the cooling island effects of water body: a case study of Shanghai, China. Ecol. Indic. 67, 31–38. https://doi.org/10.1016/j.ecolind.2016.02.040.
Dugord, P.-A., Lauf, S., Schuster, C., Kleinschmit, B., 2014. Land use patterns, temperature distribution, and potential heat stress risk – the case study Berlin, Germany. Comput. Environ. Urban Syst. 48, 86–98.
Ellison, D., Morris, C.E., Locatelli, B., Sheil, D., Cohen, J., 2017. Trees, forests and water: cool insights for a hot world. Glob. Environ. Chang. 43, 51–61.
Fan, H.Y., Yu, Z.W., Yang, G.Y., Liu, T.Y., 2019. How to cool hot-humid (Asian) cities with urban trees? An optimal landscape size perspective. Agric. For. Meteorol. 265, 338–348. https://doi.org/10.1016/j.agrformet.2018.11.027.
Feng, W., Ding, W., Zhen, M., Zou, W., Wang, H., 2021. Cooling effect of urban small green spaces in Qujiang campus, Xi'an Jiaotong University China. Environ. Dev. Sustain. 24, 4278–4298.
Feyisa, G.L., Dons, K., Meilby, H., 2014. Efficiency of parks in mitigating urban heat island effect: an example from Addis Ababa. Landsc. Urban Plan. 123, 87–95. https://doi.org/10.1016/j.landurbplan.2013.12.008.
Gabriel, K.M.A., Endlicher, W.R., 2011. Urban and rural mortality rates during heat waves in Berlin and Brandenburg, Germany. Environ. Pollut. 159, 2044–2050.
Gilbert, H., Mandel, B.H., Levinson, R., 2016. Keeping California cool: recent cool community developments. Energy Build 114, 20–26.
Gomez-Martinez, F., de Beurs, K.M., Koch, J., Widener, J., 2021. Multi-temporal land surface temperature and vegetation greenness in urban green spaces of Puebla, Mexico. Land 10, 1–25.
Grimm, N.B., Faeth, S.H., Golubiewski, N.E., Redman, C.L., Wu, J., 2008. Global change and the ecology of cities. Science (80-.) 319, 756–760.
Gunawardena, K.R., Wells, M.J., Kershaw, T., 2017. Utilising green and bluespace to mitigate urban heat island intensity. Sci. Total Environ. 584–585, 1040–1055.
Hathway, E.A., Sharples, S., 2012. The interaction of rivers and urban form in mitigating the urban Heat Island effect: a UK case study. Build. Environ. 58, 14–22.

He, B., Zhu, J., 2018. Constructing community gardens? Residents' attitude and behaviour towards edible landscapes in emerging urban communities of China. Urban For. Urban Green. 34, 154–165.
Hoag, H., 2015. How cities can beat the heat. Nature 524, 402–404.
Hsiang, S.M., Meng, K.C., Cane, M.A., 2011. Civil conflicts are associated with the global climate. Nature 476, 438–441.
Jiménez-Muñoz, J.C., Sobrino, J.A., Skoković, D., Mattar, C., Cristóbal, J., 2014. Land surface temperature retrieval methods from Landsat-8 thermal infrared sensor data. IEEE Geosci. Remote Sens. Lett. 11, 1840–1843.
Jin, M., Dickinson, R.E., Zhang, D.-L., 2005. The footprint of urban areas on global climate as characterized by MODIS. J. Clim. 18, 1551–1565.
Koc, C.B., Osmond, P., Peters, A., 2018. Evaluating the cooling effects of green infrastructure: a systematic review of methods, indicators and data sources. Sol. Energy 166, 486–508.
Kong, F., Yin, H., James, P., Hutyra, L.R., He, H.S., 2014. Effects of spatial pattern of greenspace on urban cooling in a large metropolitan area of eastern China. Landsc. Urban Plan. 128, 35–47. https://doi.org/10.1016/j.landurbplan.2014.04.018.
Kusaka, H., Hara, M., Takane, Y., 2012. Urban climate projection by the WRF model at 3 km horizontal grid increment: dynamical downscaling and predicting heat stress in the 2070's august for Tokyo, Osaka, and Nagoya. J. Meteorol. Soc. Jpn. 90b, 47–63.
Li, D., Bou-Zeid, E., 2013. Synergistic interactions between urban Heat Islands and heat waves: the 1 impact in cities is larger than the sum of its parts. J. Appl. Meteorol. Climatol. 52, 2051–2064.
Li, Y., Zhao, M., Motesharrei, S., Mu, Q., Kalnay, E., Li, S., 2015. Local cooling and warming effects of forests based on satellite observations. Nat. Commun. 6, 6603.
Lin, W., Yu, T., Chang, X., Wu, W., Zhang, Y., 2015. Calculating cooling extents of green parks using remote sensing: method and test. Landsc. Urban Plan. 134, 66–75. https://doi.org/10.1016/j.landurbplan.2014.10.012.
Manteghi, G., Limit, H., Remaz, D., 2015. Water bodies an urban microclimate: A review. Mod. Appl, Sci, p. 9.
Masoudi, M., Tan, P.Y., 2019. Multi-year comparison of the effects of spatial pattern of urban green spaces on urban land surface temperature. Landsc. Urban Plan. 184, 44–58. https://doi.org/10.1016/j.landurbplan.2018.10.023.
McGeehin, M.A., Mirabelli, M., 2001. The potential impacts of climate variability and change on temperature-related morbidity and mortality in the United States. Environ. Health Perspect. 109, 185–189.
Mora, C., Dousset, B., Caldwell, I.R., Powell, F.E., Geronimo, R.C., 2017. Global risk of deadly heat. Nat. Clim. Chang. 7, 501–506.
Murakawa, S., Sekine, T., Narita, K., Nishina, D., 1991. Study of the effects of a river on the thermal environment in an urban area. Energy Build. 16, 993–1001.
Myint, S.W., Zheng, B., Talen, E., Fan, C., Kaplan, S., Middel, A., Smith, M., Huang, H.-P., Brazel, A., 2015. Does the spatial arrangement of urban landscape matter? Examples of urban warming and cooling in Phoenix and Las Vegas. Ecosyst. Health Sustain. 4, 13–28.
Oke, T.R., 1982. The energetic basis of the urban heat island. Q. J. R. Meteorol. Soc. 108, 1–24. https://doi.org/10.1002/qj.49710845502.
Peng, J., Dan, Y., Qiao, R., Liu, Y., Dong, J., Wu, J., 2021. How to quantify the cooling effect of urban parks? Linking maximum and accumulation perspectives. Remote Sens. Environ. 252, 112135.
Rahman, M.A., Moser, A., Rötzer, T., Pauleit, S., 2017. Microclimatic differences and their influence on transpirational cooling of Tilia cordata in two contrasting street canyons in MunichGermany. Agric. For. Meteorol. 232, 443–456.
Rizwan, A.M., Dennis, L.Y.C., Liu, C., 2008. A review on the generation, determination and mitigation of urban Heat Island. J. Environ. Sci. 20, 120–128. https://doi.org/10.1016/S1001-0742(08)60019-4.
Santamouris, M., Ban-Weiss, G., Osmond, P., Paolini, R., 2018. Progress in urban greenery mitigation science–assessment methodologies advanced technologies and impact on cities. J. Civ. Eng. Manag. 24, 638–671.
Schwaab, J., Meier, R., Mussetti, G., Seneviratne, S., Bürgi, C., Davin, E.L., 2021. The role of urban trees in reducing land surface temperatures in European cities. Nat. Commun. 12, 6763.
Shi, D., Song, J., Huang, J., Zhuang, C., Guo, R., Gao, Y., 2020. Synergistic cooling effects (SCEs) of urban green-blue spaces on local thermal environment: a case study in Chongqing, China. Sustain. Cities Soc. 55, 102065.
Shiflett, S.A., Liang, L.L., Crum, S.M., Feyisa, G.L., Wang, J., Jenerette, G.D., 2017. Variation in the urban vegetation, surface temperature, air temperature nexus. Sci. Total Environ. 579, 495–505. https://doi.org/10.1016/j.scitotenv.2016.11.069.
Stewart, I.D., Oke, T.R., 2003. Local climate zones for urban temperature studies. Bull. Am. Meteorol. Soc. 86, 370–384.
Sun, R., Chen, L., 2012. How can urban water bodies be designed for climate adaptation? Landsc. Urban Plan. 105, 27–33. https://doi.org/10.1016/j.landurbplan.2011.11.018.
Sun, R., Chen, A., Chen, L., Lü, Y., 2012. Cooling effects of wetlands in an urban region: the case of Beijing. Ecol. Indic. 20, 57–64.
Suzhou Local Chronicles Compilation Office, 2022. Suzhou Chronicles: Nature Environment. in Chinese Accessed May 9, 2022 http://dfzb.suzhou.gov.cn/dfzb/zrdl/202205/700ee4a4856147d1b789921c8cc7c856.shtml.
Suzhou Municipal Bureau Statistics, 2020. Suzhou Statistical Yearbook 2020. in Chinese. https://www.suzhou.gov.cn/sztjj/tjnj/2020/zk/indexce.htm. (Accessed 9 January 2022).
Theeuwes, N.E., Solcerová, A., Steeneveld, G.J., 2013. Modeling the influence of open water surfaces on the summertime temperature and thermal comfort in the city. J. Geophys. Res. Atmos. 118, 8881–8896.
United Nations Department of Economic and Social Affairs, 2019. World Urbanization Prospects: The 2018 Revision. in ChineseUnited Nations Publications.
Wang, Y., Ouyang, W., 2021. Investigating the heterogeneity of water cooling effect for cooler cities. Sustain. Cities Soc. 75, 103281.
Weng, Q., Rajasekar, U., Hu, X., 2011. Modeling urban heat islands and their relationship with impervious surface and vegetation abundance by using ASTER images. IEEE Trans. Geosci. Remote Sens. 49, 4080–4089. https://doi.org/10.1109/TGRS.2011.2128874.
Wong, P.P.-Y., Lai, P.-C., Low, C.-T., Chen, S., Hart, M., 2016. The impact of environmental and human factors on urban heat and microclimate variability. Build. Environ. 95, 199–208.
Wu, D., Wang, Y., Fan, C., Xia, B., 2018. Thermal environment effects and interactions of reservoirs and forests as urban blue-green infrastructures. Ecol. Indic. 91, 657–663.
Wu, J., Li, C., Zhang, X., Zhao, Y., Liang, J., Wang, Z., 2020. Seasonal variations and main influencing factors of the water cooling islands effect in Shenzhen. Ecol. Indic. 117, 106699.
Xue, Z., Hou, G., Zhang, Z., Lyu, X., Jiang, M., Zou, Y., Shen, X., Wang, J., Liu, X., 2019. Quantifying the cooling-effects of urban and peri-urban wetlands using remote sensing data: case study of cities of Northeast China. Landsc. Urban Plan. 182, 92–100.
Yan, H., Wu, F., Dong, L., 2018. Influence of a large urban park on the local urban thermal environment. Sci. Total Environ. 622, 882–891. https://doi.org/10.1016/j.scitotenv.2017.11.327.
Yang, G., Yu, Z., Jørgensen, G., Vejre, H., 2020. How can urban blue-green space be planned for climate adaption in high-latitude cities? A seasonal perspective. Sustain. Cities Soc. 53, 101932.
Yu, Z., Guo, X., Jørgensen, G., HenrikVejre, 2017. How can urban green spaces be planned for climate adaptation in subtropical cities? Ecol. Indic. 82, 152–162.
Yu, Z., Guo, X., Zeng, Y., Koga, M., Vejre, H., 2018. Variations in land surface temperature and cooling efficiency of green space in rapid urbanization: the case of Fuzhou city, China. Urban For. Urban Green 29, 113–121.
Yu, Z., Yang, G., Zuo, S., Jørgensen, G., Koga, M., Vejre, H., 2020. Critical review on the cooling effect of urban blue-green space: a threshold-size perspective. Urban For. Urban Green. 49, 126630.
Yu, Z., Zhang, J., Yang, G., Schlaberg, J., 2021. Reverse thinking: a new method from the graph perspective for evaluating and mitigating regional surface Heat Islands. Remote Sens. 13, 1127.
Zhang, Y., Murray, A.T., Turner II, B.L., 2017. Optimizing green space locations to reduce daytime and nighttime urban heat island effects in Phoenix, Arizona. Landsc. Urban Plan. 165, 162–171.
Zhao, Z.-Q., He, B.-J., Li, L.-G., Wang, H.-B., Darko, A., 2017. Profile and concentric zonal analysis of relationships between land use/land cover and land surface temperature: case study of ShenyangChina. Energy Build. 155, 282–295.
Zhao, L., Oppenheimer, M., Zhu, Q., Baldwin, J.W., Ebi, K.L., Bou-Zeid, E., Guan, K., Liu, X., 2018. Interactions between urban heat islands and heat waves. Environ. Res. Lett. 13. https://doi.org/10.1088/1748-9326/aa9f73.
Zheng, Y., Li, Y., Hou, H., Murayama, Y., 2021. Quantifying the cooling effect and scale of large Inner-City lakes based on landscape patterns: a case study of Hangzhou and Nanjing. Remote Sens. 13, 1526.
Zhou, W., Cao, F., Wang, G., 2019a. Effects of spatial pattern of forest vegetation on urban cooling in a compact megacity. Forests 10, 282. https://doi.org/10.3390/f10030282.
Zhou, W., Shen, X., Cao, F., Sun, Y., 2019. Effects of area and shape of greenspace on urban cooling in Nanjing, China. J. Urban Plan. Dev. https://doi.org/10.1061/(ASCE)UP.1943-5444.0000520.
Zhou, Y., Gao, W., Yang, C., Shen, Y., 2021. Exploratory analysis of the influence of landscape patterns on lake cooling effect in WuhanChina. Urban Clim. 39, 100969.
Zhou, W., Yu, W., Wu, T., 2022. An alternative method of developing landscape strategies for urban cooling: a threshold-based perspective. Landsc. Urban Plan. 225, 104449.